Plant Physiology and Biochemistry 135 (2019) 19–29

Contents lists available at ScienceDirect

Plant Physiology and Biochemistry

journal homepage: www.elsevier.com/locate/plaphy

Research article

RrGT1, a key gene associated with anthocyanin biosynthesis, was isolated from *Rosa rugosa* and identified via overexpression and VIGS

Xiaoming Sui[1], Mingyuan Zhao[1], Xu Han, Lanyong Zhao*, Zongda Xu**

College of Forestry, Shandong Agricultural University, 61 Daizong Street, Taian, 271018, China

ARTICLE INFO

Keywords:
Rosa rugosa
RrGT1 gene
Clone
Overexpression
VIGS
Anthocyanin

ABSTRACT

At present, research on the flower color of *Rosa rugosa* requires very innovative and practical studies. Glycosylation plays an important role in increasing the stability and solubility of anthocyanins in plants. In this study, a gene with a full-length cDNA of 1161 bp encoding 386 amino acids, designated *RrGT1* (MK034140), was isolated from the flowers of *R. rugosa* 'Zizhi' and then functionally characterized. Sequence alignment revealed that the coding regions of *RrGT1* were highly specific among different species but still contained typical conserved amino acid residues that are crucial for *RrGT1* enzyme activity. *RrGT1* transcripts were detected in various tissues of *R. rugosa* 'Zizhi' and *Rosa davurica*, and their expression patterns corresponded with the accumulation of anthocyanins. Additionally, the *in vivo* function of *RrGT1* was investigated via its overexpression in *Arabidopsis thaliana*. Transgenic *Arabidopsis* plants expressing *RrGT1* regained red color pigmentation of their leaves and flower stems, indicating that *RrGT1* could encode a functional glycosyltransferase (GT) protein for anthocyanin biosynthesis and could function in other species. The functional verification of *RrGT1* for anthocyanin biosynthesis in *R. rugosa* was performed via virus-induced gene silencing (VIGS). This was the first time that a VIGS system was developed for use with perennial *Rosa* plants grown naturally in the field as experimental materials to study a key color-controlling gene in *Rosa*. When the *RrGT1* gene was silenced, the *Rosa* plants displayed a pale petal color phenotype. The detection results showed that the expression of the endogenous *RrGT1* gene was significantly downregulated while the six key structural genes in its upstream were normally expressed, and the contents of all anthocyanins also decreased significantly. Therefore, we speculated that glycosylation of *RrGT1* plays a crucial role in anthocyanin biosynthesis in *R. rugosa*.

1. Introduction

Rosa rugosa is an important ornamental plant species that belongs to the genus *Rosa* in the family *Rosaceae*. This species is native to China and is widely distributed worldwide. Because of its unique fragrance, color, cold resistance and drought resistance, there is great potential for the development of this species for use in garden applications. Many varieties of roses exist, but most of them are traditional colors such as pink and purple. A few varieties are white, and some lack yellow, bright red, orange and compound colors, etc. (Feng et al., 2009). Therefore, the development of innovative rose colors has become the main goal of breeders. Analysis of the pigment composition of rose and the study of the expression characteristics of the key genes encoding enzymes that catalyze the synthesis of rose pigments were important prerequisites for molecular breeding of rose color traits (Chen et al., 2010). Anthocyanins determine the color of higher plant organs. Structural genes (*CHS*, *CHI*, *F3H*, *F3'H*, *DFR*, *ANS*, *3GT*, etc.) and regulatory genes (*MYB*, mostly *R2R3 MYB*, *BHLH* and *WD40* classes) related to the anthocyanin biosynthesis pathway have been cloned and sequenced, and related protein functional studies have been performed in many plant species, such as petunia, maize, snapdragon and so on. However, less anthocyanin-related research has been conducted in roses than in those species.

Anthocyanins, derived from the anthocyanin biosynthesis pathway, were the largest group of water-soluble plant flavonoids found in organs of plants and crops (Holton and Cornish, 1995; Kim et al., 2003;

Abbreviations: cDNA, complementary DNA; RACE, rapid amplification of cDNA ends; CDS, coding DNA sequence; AS, acetosyringone; PCR, polymerase chain reaction; qRT-PCR, quantitative real-time polymerase chain reaction; VIGS, virus-induced gene silencing; HPLC, high-performance liquid chromatography

* Corresponding author.
** Corresponding author.
E-mail addresses: sdzly369@163.com (L. Zhao), xuzoda@163.com (Z. Xu).
[1] These authors contribute equally.

https://doi.org/10.1016/j.plaphy.2018.11.022
Received 5 August 2018; Received in revised form 29 October 2018; Accepted 19 November 2018
Available online 22 November 2018
0981-9428/

Martens et al., 2010). Anthocyanins were unstable in plants; they existed mainly in the form of glycosides within the vacuole (Ge et al., 2012). The flavonoid 3-*O*-glycosyltransferase (*3GT*) gene lies downstream in the anthocyanin synthesis pathway. The enzyme coded by this gene could catalyze the glycosylation of UDP-glucose to replace the 3 hydroxyl groups of anthocyanin molecules and cause anthocyanin glycosylation to produce colored and stable anthocyanins. Glycosylation could change the hydrophilicity, biochemical activity and subcellular localization of anthocyanins, which is beneficial to their transport and storage in cells and organisms (Vogt and Jones, 2000).

Studies have shown that the *3GT* gene was expressed only in red grape (*Vitis vinifera*) varieties and not in white grape ones. When a *3GT* transgene was transformed into a colorless embryo, a pale-red bud was produced (Kobayashi et al., 2001; Li and Yu, 2003). Studies by Afifi et al. on the expression of five key genes involved in anthocyanin synthesis in grape cell tissue indicate that the presence of cytotoxic factors of eutypine inhibited the expression of *3GT* and thus reduced the content of anthocyanins (Afifi et al., 2003). This finding indicated that *3GT* was the key gene in grape skin color (from white to red) and was also a key gene in the anthocyanin biosynthesis pathway (Boss et al., 1996). In *Gentiana triflora*, *3GT* gene expression was detected mostly in blue petals and rarely in white flowers (Nakatsuka et al., 2005). Expression of the *3GT* gene was very important for anthocyanin accumulation in many plant species, and its expression intensity was positively correlated with anthocyanin synthesis (Ju, 1995).

In this study, we cloned and identified the *RrGT1* gene from the petals of *R. rugosa* for the first time. We carried out detailed bioinformatics analysis and homology analysis of the *RrGT1* gene. Stable transformation of the *RrGT1* gene showed that its overexpression was positively correlated with the accumulation of anthocyanins in *Arabidopsis*. VIGS results in mature *Rosa* plants under field conditions also confirmed this conclusion. We verified functions of the *RrGT1* gene in anthocyanin metabolism in both the positive and negative directions to provide useful information for subsequent color-improvement projects in *R. rugosa*.

2. Materials and methods

2.1. Plant materials

With respect to *Rosa*, *R. rugosa* 'Zizhi' and *R. davurica* plants cultivated in the rose germplasm nursery of Shandong Agricultural University were used as test material. We collected petals at the budding stage, initial opening stage, half opening stage, full opening stage and wilting stage as well as seven different tissue samples (roots, stems, leaves, petals at the budding stage, sepals, stamens and pistils) in the mornings of sunny days from 20 April to 10 May 2017. After flash freezing in liquid nitrogen, all samples, which were collected in triplicate, were put into a −80 °C refrigerator for storage.

For *Arabidopsis thaliana*, the Columbia ecotype was used as transgenic material. After disinfection, the seeds were sown in Murashige and Skoog (MS) solid medium (without antibiotics). After 3 days of vernalization at 4 °C in darkness, the seeds were placed in a growth chamber (25 °C, 16 h/23 °C, 8 h day/night, 60% relative humidity) for approximately 7–10 days. After two true leaves were present, the seedlings were transferred into small flowerpots that contained substrate, and the original temperature, humidity and illumination conditions were maintained.

2.2. Extraction of total RNA and synthesis of first-strand cDNA

The total RNA was extracted via an EASY Spin Plant RNA Rapid Extraction Kit (Aidlab Biotech, Beijing, China) in accordance with the manufacturer's specifications. The integrity of the RNA was measured by gel electrophoresis with 1.0% nondenatured agarose, the purity and concentration of the RNA were detected by a Nanodrop 2000C ultramicrospectrophotometer (Thermo Fisher Scientific, Wilmington, Delaware, USA), and the qualified RNA was preserved at −80 °C. First-strand cDNA was synthesized via a 5 × All-In-One RT MasterMix Reverse Transcription Kit (ABM Company, Vancouver, Canada) in accordance with both the manufacturer's protocol and the requirements of RT-PCR and qRT-PCR.

2.3. Cloning of the full-length CDS of the RrGT1 gene

We identified the *RrGT1* gene that contained the complete 5′ CDS from the *R. rugosa* transcriptome data in our laboratory. The cDNA 3′ terminal sequence of the target gene was then amplified by 3'-RACE technology as same as that in the report of Han et al. (2017). Primers *RrGT1*-F and *RrGT1*-R (Table S1) were designed and amplified according to the full-length cDNA sequence of the *RrGT1* gene.

2.4. A. thaliana stable transformation

The plasmids of a *pCAMBIA1304* vector and *RrGT1* gene with restriction sites (*SpeI* and *BstEII*) were extracted and digested by double enzymes. The digestion products were then ligated with DNA ligase (Fig. S1A) and transformed into *Agrobacterium tumefaciens*.

A. tumefaciens inflorescence infection was used to transform *A. thaliana*. The prepared *A. tumefaciens* infection solution (OD_{600} = 0.4, containing 5% sucrose and 0.01% Silwet L-77; a *pCAMBIA1304* empty carrier served as the control) was poured into petri dishes, and the whole inflorescence was immersed in the solution for 10 s. After infection, the plants were subjected to a dark treatment for 12 h, after which they were allowed to grow normally. One week later, an additional floral dip was performed in the same way. Mature T_0 seeds were collected, disinfected, and then sown on MS medium that contained hygromycin to screen the transformants. The resistant plants grew normally; they were removed and transplanted into small flowerpots.

2.5. VIGS in Rosa

Based on a modified TRV-GFP vector, a TRV-GFP-*RrGT1* recombinant viral vector was constructed. pTRV1 and pTRV2-GFP are two RNA strands of the TRV-GFP virus vector, and the multiple cloning sites are mainly on pTRV2-GFP. For silencing *RrGT1* specifically in *R. rugosa*, a 543 bp fragment of the *RrGT1* gene was amplified and cloned into pTRV2-GFP (Fig. S2A).

The pTRV1, pTRV2-GFP and pTRV2-GFP-*RrGT1* plasmids were transformed into *A. tumefaciens*, which were then cultured in YEB medium that contained kanamycin, rifampicin and AS at 28 °C for 14–16 h until an OD_{600} = 1.5 was reached. Before infection, pTRV1 was added to the infection liquid that contained pTRV2-GFP and pTRV2-GFP-*RrGT1* in equal volume; the solution was subsequently mixed, forming a complete TRV-GFP and TRV-GFP-*RrGT1* virus carrier. The mixed bacterial solution was kept at room temperature in darkness for 4 h (Bachan and Dinesh-Kumar, 2012; Burch-Smith et al., 2006; Chen et al., 2004; Jiang et al., 2011; Liu et al., 2002; Quadrana et al., 2011).

Perennial *Rosa* plants that grew naturally in the field were used as experimental materials, and the experimental treatment time was approximately one month before *R. rugosa* flowering. Because the leaves and twigs were difficult to inject with syringes and because vacuum infiltration could not be used in the field, we used the method of first scratching leaves and twigs and then infecting with *A. tumefaciens*. To improve the infection efficiency, 0.01% Silwet L-77 was added to the infection liquid, and the plants were subjected to darkness for 24 h after infection for 10 min.

The detection and imaging of the visualized GFP after VIGS treatment were performed at night with a handheld high-intensity ultraviolet lamp (Model SB-100P/F; Spectronics Corporation, Westbury, New York, USA) and a Nikon D90 camera, respectively.

2.6. qRT-PCR detection

We analyzed the gene expression by qRT-PCR on a Bio-Rad CFX96™ Real-Time PCR instrument (Bio-Rad, Inc., USA). The qRT-PCR mixture (total volume of 20 μL) contained 10 μL of SYBR® Premix Ex Taq™ (TaKaRa, Inc., Japan), 8.2 μL of ddH_2O, 0.4 μL of each primer and 1 μL of cDNA. The PCR program consisted of an initial step of 95 °C for 30 s; 40 cycles of 95 °C for 5 s and 60 °C for 30 s; and then a dissociation stage of 95 °C for 10 s, 65 °C for 5 s and 95 °C for 5 s. Each gene was assessed via three biological replicates. The relative expression levels of the genes were calculated by the $2^{-\Delta\Delta Ct}$ method (Schmittgen and Livak, 2008).

2.7. Total anthocyanin extractions and HPLC analysis

All samples (0.1 g fresh weight) were homogenized in liquid nitrogen, after which they were extracted with 5 mL of an acidic methanol solution (70: 0.1: 29.9, v/v/v; CH_3OH: HCl: H_2O) at 4 °C in darkness for 24 h and then sonicated for 30 min. After centrifugation, each extract was passed through a membrane filter (0.22 mm). The aqueous phase was used to determine the absorbance at 530 nm and 657 nm. The total anthocyanin contents were quantified via the following equation: $Q_{Anthocyanins} = (A_{530} - 0.25 \times A_{657}) \times M^{-1}$, where $Q_{Anthocyanins}$ is the amount of anthocyanins, A_{530} and A_{657} are the absorptions at the indicated wavelengths, and M is the weight of the plant material in grams used for extraction.

Qualitative and quantitative analyses of anthocyanins were performed via HPLC. Three independent biological replicates were measured for each sample. The specific conditions of the anthocyanin analysis were the same as those in the report of Yang et al. (2015). Cy3G, Cy3G5G, Pg3G, Pg3G5G, Pn3G, Pn3G5G, Dp3G and Dp3G5G (EXTRASYNTHESE Trading Company, France) were used as references for the anthocyanin analysis.

3. Results

3.1. Cloning of RrGT1 and sequence analysis

The full-length CDS sequence of *RrGT1* (MK034140) was cloned and then confirmed by sequencing. The complete open reading frame from the ATG start codon to the TAA termination codon encodes a 386 amino acid protein (Fig. 1A). Multiple sequence alignment (Fig. 1B) revealed that the *RrGT1* protein, which belongs to the GTB superfamily, displays strong species specificity in the N-terminal region and PSPG conserved domains that consist of 44 amino acid residues in the C-terminal region. Using MEGA 5.0 software, a phylogenetic tree (Fig. 1C) was constructed from the amino acid sequences of 21 plants, including the sequence of *RrGT1*. The results showed that the homology of *RrGT1* with a GT of any other species is less than 60%, indicating that GT genes are highly variable among different species.

3.2. Temporal and spatial expression patterns of the RrGT1 gene

The expression levels of the *RrGT1* gene, which significantly differed, were assessed during five flowering stages. For *R. rugosa* 'Zizhi' (Fig. 2A), the highest expression level was observed during the full opening stage, and the lowest was observed during the budding stage. In *R. davurica* (Fig. 2B), the expression level was also highest during the full opening stage but lowest during the half opening stage. The expression patterns of the *RrGT1* gene in *R. rugosa* 'Zizhi' and *R. davurica* showed the same trend.

The expression levels of the *RrGT1* gene, which also significantly differed, were assessed in seven different tissue types. The expression level in the leaves, stems and flower buds was relatively high but was relatively low in the other tissues in both *R. rugosa* 'Zizhi' (Fig. 2C) and *R. davurica* (Fig. 2D).

3.3. Construction and verification of recombinant expression vector pCAMBIA1304-RrGT1

The vector and target gene were digested separately(Fig. S1B) and linked together according to the pre-designed vector recombination technique route (Fig. S1A). In order to verify whether the recombination was successful, we designed a pair of specific primers (Table S1) to detect the transformation results by PCR, and the results showed positive(Fig. S1C). In order to eliminate the possibility of false positivity and to further verify whether the target gene had been mutated or deleted during the recombination, we identified the target gene by double enzyme digestion and sequencing. The results of double enzyme digestion (Fig. S1D) showed that the recombinant vector was cut into two distinct fragments: one part of the original vector and the other part of the target gene. The plasmid of the empty vector was used as the control. The sequencing results also showed that there was no base mutation and deletion in the target gene fragment of the embedded vector. The results above showed that the recombinant expression vector pCAMBIA1304-*RrGT1* was constructed successfully.

3.4. Overexpression of the RrGT1 gene promoted anthocyanin accumulation in A. thaliana

After transformation, the harvested T_0 seeds were screened on MS medium that contained hygromycin, and a total of 9 plants tested positive by PCR-based detection (Fig. 3C) and PCR products sequencing. The color of the leaves (Fig. 3A) and flower stems (Fig. 3B) of the transgenic *A. thaliana* plants is clearly deeper than that of the plants in the control group and empty vector group; the change in flower stem color is especially obvious and had become purplish red. The contents of total anthocyanins in the transgenic group, empty vector group and control group were subsequently determined. The results (Fig. 3D) showed that, compared with that in the control group, the anthocyanin content in the empty vector group was basically unchanged, while the anthocyanin content in the 9 transgenic plants significantly increased.

3.5. Construction and verification of recombinant virus vector pTRV2-GFP-RrGT1

Similar to the construction process of the transgenic recombinant expression vector, the virus vector pTRV2-GFP and the specific fragment of the *RrGT1* gene were respectively digested (Fig. S2B) and then were combined together, according to the preset viral vector recombination technology route (Fig. S2A). Then the PCR (Fig. S2C)was verified by specific primers (Table S1), and the base mutation and deletion were verified by double enzyme digestion (Fig. S2D)and sequencing. All of the results above indicated that the recombinant virus vector pTRV2-GFP-*RrGT1* was successfully constructed.

3.6. VIGS of the RrGT1 gene reduced the transcript abundance of the endogenous RrGT1 gene

At 14 days after infection, GFP detection was performed on the newly grown leaves of the infected plants (TRV-GFP and TRV-GFP-*RrGT1*) and on the untreated leaves of both *Rosa* species. GFP imaging (Fig. 4A and B) showed that the leaves treated with VIGS (TRV-GFP and TRV-GFP-*RrGT1*) showed green fluorescence under longwave ultraviolet light, while the untreated leaves in the control group showed red fluorescence. The corresponding leaves were collected for semi-quantitative RT-PCR detection, and the *RrGAPDH* gene was used as an internal control (Qi, 2016) to confirm the efficiency of VIGS. The results (Fig. 4C) showed that the *TRV* and *GFP* genes could be detected in the leaves treated with VIGS (TRV-GFP and TRV-GFP-*RrGT1*), but the abundance of the *RrGT1* transcript significantly decreased only in the leaves treated with TRV-GFP-*RrGT1*; the abundance was normal in the leaves treated with TRV-GFP. In the control group, the *TRV* and *GFP*

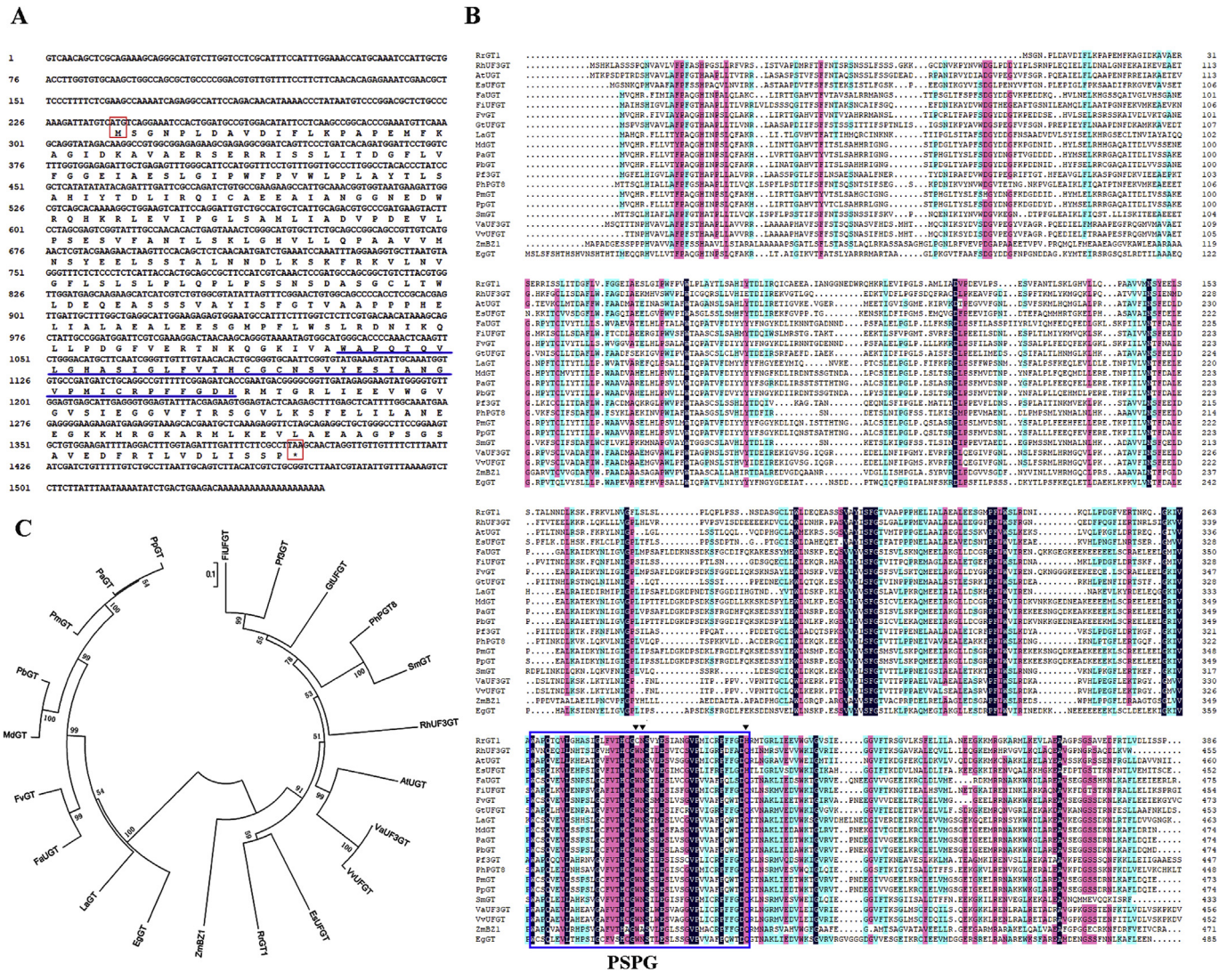

Fig. 1. Sequence analysis and phylogenetic tree analysis of the *RrGT1* gene. **(A)** cDNA sequence of *RrGT1* and its deduced amino acids. The red box shows the start codon and the termination codon and the amino acids they encode. The sequences corresponding to the outer end of the two red boxes are 5′UTR and 3′UTR, respectively. The PSPG domains were underlined by the blue line. **(B)** Amino acid sequences homologous analysis of the *RrGT1* gene and other species related genes. Alignments were performed using DNAMAN (version 6.0). The relative genes of 21 species including the *RrGT1* gene were selected for comparative analysis. The blue box shows the PSPG domains. Black triangles (from left to right) indicate 22, 23 and 44 amino acids in the PSPG box. **(C)** Phylogenetic tree of *RrGT1* and GT members from other plant species. The tree was constructed by neighbor-joining method using MEGA 5.0 software. Branch numbers represent as percentage of bootstrap values in 1000 sampling replicates and scale indicates branch lengths. (For interpretation of the references to color in this figure legend, the reader is referred to the Web version of this article.)

genes were not detected, and the *RrGT1* gene was expressed normally.

At 30–40 days after infection, the control group and TRV-GFP group definitively showed no obvious changes in flower color, but the petals in the TRV-GFP-*RrGT1* group were clearly lighter in color. GFP imaging and qRT-PCR were then performed on the blossoming petals of untreated plants and infected plants (TRV-GFP and TRV-GFP-*RrGT1*) of both *Rosa* species. The results were as expected: the petals treated with VIGS (TRV-GFP and TRV-GFP-*RrGT1*) showed green fluorescence under longwave ultraviolet light, while the petals in the control group showed red fluorescence (Fig. 5A and B). The results of qRT-PCR (Fig. 5C) were consistent with those of the above detection. In both *Rosa* species, the relative expression trends of the *RrGT1* gene were also essentially consistent: the relative expression of the *RrGT1* gene in the TRV-GFP group was essentially the same as that in the control group. However, the transcript abundance of the endogenous *RrGT1* gene in the petals treated with TRV-GFP-*RrGT1* was significantly downregulated.

3.7. The decrease of anthocyanin accumulation in Rosa petals was related to VIGS of RrGT1

In order to further clarify the role of the post transcriptional silencing of the *RrGT1* gene in the outcome of the current color change, we compared the relative expression of the six key structural genes, *RrCHS* (KT809351), *RrCHI* (KT809352), *RrF3H* (KT809354), *RrF3′H* (MG735186), *RrDFR* (KT809350) and *RrANS* (KT809353), in the upstream of the *RrGT1* gene in the anthocyanin pathway. The results (Fig. 6) showed that the relative expression of the six genes in control group, TRV-GFP group and TRV-GFP-*RrGT1* group of *R. rugosa* ‘Zizhi’ and *R. davurica* had no obvious change. Therefore, the effects of upstream structure genes can be basically excluded. And it is speculated that the change of flower color after VIGS treatment was related to the post transcriptional silencing of *RrGT1* gene.

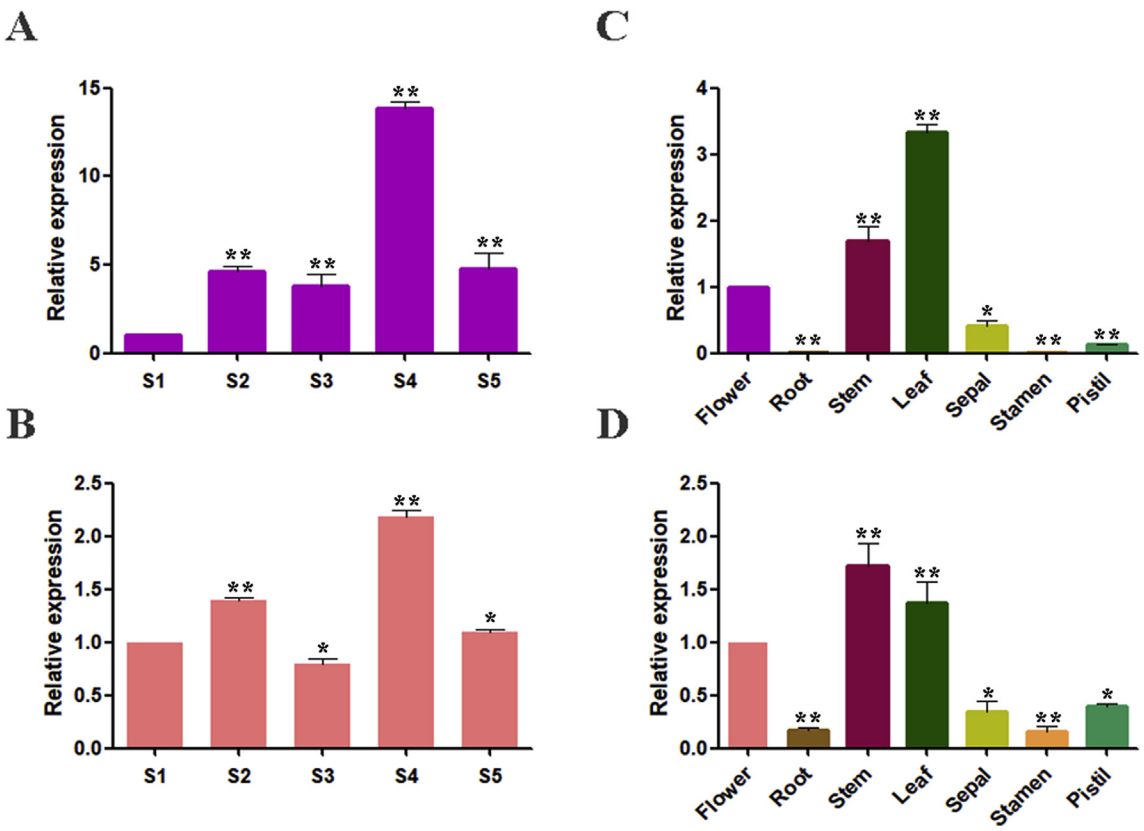

Fig. 2. Temporal and spatial expression patterns of *RrGT1*. Relative expression of the *RrGT1* gene during five flowering stages of *R. rugosa* 'Zizhi' **(A)** and *R. davurica* **(B)**. S1, budding stage; S2, initial opening stage; S3, half opening stage; S4, full opening stage; S5, wilting stage. Relative expression of the *RrGT1* gene in seven different tissues of *R. rugosa* 'Zizhi' **(C)** and *R. davurica* **(D)**. The error bars represent the SDs of triplicate reactions. The experiment was repeated three times, and each yielded similar results. *P < 0.05 and **P < 0.01 indicate significant differences between different flowering stages and between different tissue types.

3.8. HPLC analysis

The anthocyanin HPLC chromatograms for *R. rugosa* 'Zizhi' (Fig. 5D) and *R. davurica* (Fig. 5E) show that the components were well separated. Comparisons with standards allow the contents of different substances to be calculated by their peak area (Table 1). For 'Zizhi', six kinds of anthocyanins were detected: Cy3G5G, Pg3G5G, Cy3G, Pn3G5G, Pg3G, and Pn3G. Pn3G5G had the highest content, while Cy3G5G had the second highest; the contents of the other four anthocyanins were relatively low. In response to VIGS treatment, reductions in the contents of several anthocyanins compared with those in the control group and TRV-GFP group were obvious. Pn3G5G exhibited the greatest drop in content, followed by Cy3G5G; the content in Pg3G was no longer detectable. For *R. davurica*, the six anthocyanins listed above were also detected. However, Cy3G5G had the highest content, and Cy3G had the second highest content; the contents of the other four anthocyanins were relatively low. In response to VIGS treatment, reductions in the contents of the six anthocyanins compared with those in the control group and TRV-GFP group were obvious. Cy3G5G exhibited the greatest drop in content, followed by Cy3G; no detection of Pn3G was observed.

4. Discussion

Although many genes have been reported to regulate the formation of flower color, there are few reports on downstream structural genes such as GTs. The final formation of anthocyanins depends on the glycosylation of GTs, so it is very important to determine the function and influence of the *RrGT1* gene in *Rosa* color formation. In this study, we successfully cloned the *RrGT1* gene, which had a full-length cDNA of 1161 bp and encoded 386 amino acids, from the petals of *R. rugosa* 'Zizhi'.

The amino acid sequence alignment between *RrGT1* and GTs from 21 other species indicated that *RrGT1* possessed a common PSPG motif of the GT superfamily (Fig. 1B). Previous studies have shown that the conserved PSPG region is related to the substrate recognition and catalytic activity of protein enzymes (Wang et al., 1993; Zhang and Xue, 2001; Kubo et al., 2004; Broothaerts et al., 2005; Herrera-Estrella and Simpson, 2005; Wang, 2009; Yonekura-Sakakibara and Hanada, 2011). If the 44 amino acids of the PSPG domain were numbered, those at positions 22, 23 and 44 play an important role in the selection of enzyme proteoglycan donors. In the PSPG domain of the *RrGT1* gene, the amino acids at positions 22, 23 and 44 are cysteine (Cys, C), asparagine (Asn, N) and histidine (His, H), respectively. Therefore, we speculate that the *RrGT1* gene uses UDP-glucose or galactose as the main glycosyl donor but has no glucuronyltransferase activity (Modolo et al., 2009).

The expression of the *RrGT1* gene during flower development and in different tissues was investigated. The expression of the *RrGT1* gene showed different trends during different flowering periods, indicating that the expression of the *RrGT1* gene was developmentally regulated during the anthocyanin biosynthesis process. The tissue-specific anthocyanin expression was similar to that of *F3GT* genes in peach, where the expression level was greatest in tissues with pigment accumulation but relatively low in unpigmented organs (Cheng et al., 2014). Notably, the stems of both *Rosa* species were purple, which is consistent with the high expression level of the *RrGT1* gene in those stems. Interestingly, *R. davurica* is one of the parents of *R. rugosa* 'Zizhi', so we speculate that this reason might explain the similar expression patterns between both *Rosa* species. In addition, *RrGT1* was highly expressed in the leaves of both *Rosa* species, so we infer that *RrGT1* is also involved in the glycosylation of secondary metabolites in leaves and plays an important role.

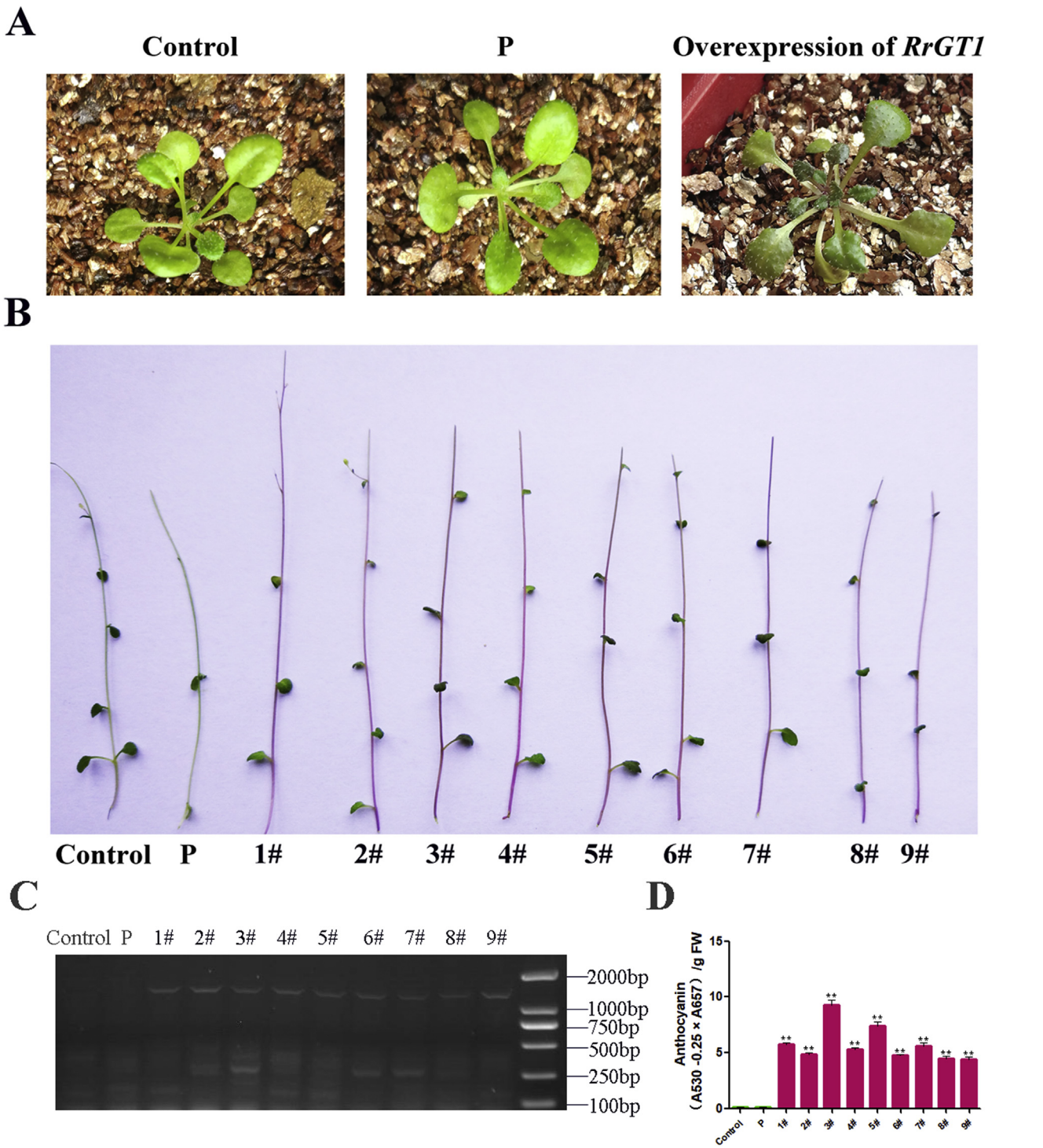

Fig. 3. Validation of transgenic *A. thaliana* plants. **(A)** Color contrast of leaves. **(B)** Color contrast of flower stems. **(C)** PCR detection in controls (empty vectors) (P) and *RrGT1 A. thaliana* transplants. **(D)** Total anthocyanin content. The error bars represent the SDs of triplicate reactions. The experiment was repeated three times, and each yielded similar results. ** indicate a significant difference from that of Control at $p < 0.01$, by Student's *t*-test. (For interpretation of the references to color in this figure legend, the reader is referred to the Web version of this article.)

In plant secondary metabolism, numerous glycosides have already been isolated as biologically active compounds and some of them have been widely used as important medicines. Glycosyltransferases usually act in the final stages of plant secondary metabolism and are used for stabilizing and solubilizing various low-molecular-mass compounds, such as flower pigments (Brugliera et al., 1994; Kroon et al., 1994), and for regulating the action of functional compounds, such as plant hormones (Szerszen et al., 1994; Martin et al., 1999, 2001). To date, most studies on the characteristics of GT enzymes have been derived from recombinant proteins produced in bacterial cells and characterized *in vitro*. However, very few published studies exist on the characterization of GTs *in vivo*. To investigate the function of the *RrGT1* gene in anthocyanin biosynthesis *in vivo*, *RrGT1* was first transferred into *A. thaliana*, which resulted in purple coloration of *A. thaliana* leaves and flower stems. Exogenous *RrGT1* enzymes can also affect the synthesis of anthocyanins in different species. In other words, the function of *RrGT1*

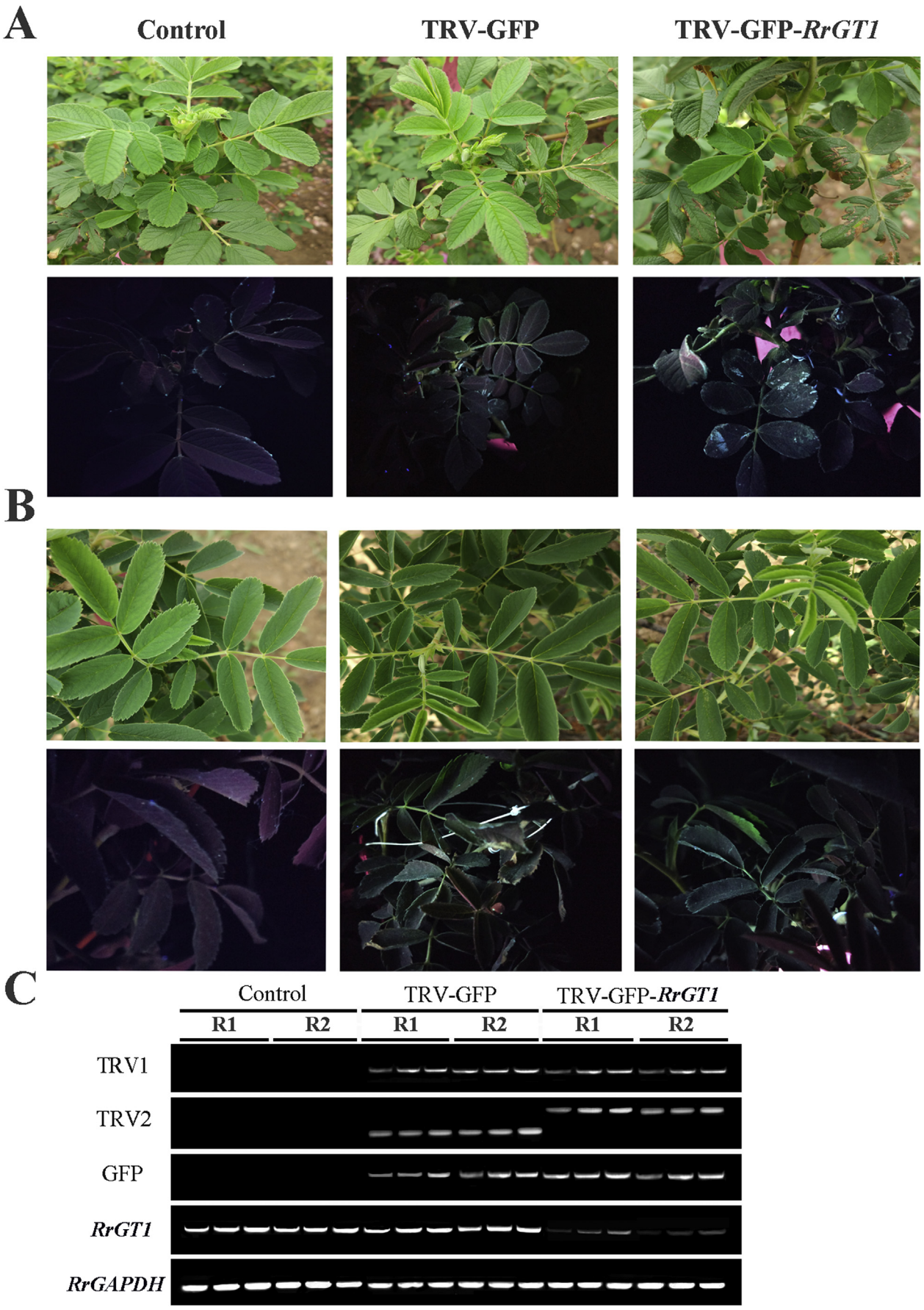

(caption on next page)

Fig. 4. Validation of VIGS in leaves. Contrast between control leaves and VIGS-treated leaves (TRV-GFP and TRV-GFP-*RrGT1*) of *R. rugosa* 'Zizhi' **(A)** and *R. davurica* **(B)**. The plants were imaged under ultraviolet illumination and normal light. **(C)** Semiquantitative RT-PCR of *TRV1*, *TRV2*, *GFP*, and *RrGT1* in control and VIGS-treated leaves. R1, *R. rugosa* 'Zizhi'; R2, *R. davurica*. *RrGAPDH* was used as an internal control. The *TRV2* fragment was larger in plants infected by TRV-GFP-*RrGT1* due to the inserted *RrGT1* fragment.

in anthocyanin biosynthesis can be exchanged among different plant species.

In this study, functions of the *RrGT1* gene have been preliminarily proven via transgenic experiments, but the results reflect only the functional verification of the *RrGT1* gene as an exogenous gene in species other than *R. rugosa*. To further clarify the role of *RrGT1* in the formation of *R. rugosa* color, we used the VIGS technique to specifically silence the *RrGT1* gene in both *Rosa* species as well as to detect and analyze the phenotypes of the flowers. The VIGS system, which involves TRV1 and TRV2, is a powerful tool for the functional characterization of genes *in vivo* (Sun et al., 2016). At present, few reports exist about the use of the VIGS system in plant floral organs, and most of the tested species belong to the Solanaceae family. For example, VIGS technology was used to study the genes controlling floral fragrance in *Petunia hybrida* (Spitzer et al., 2007), and the roles of the *SlMADSI*, *NbMADS4-1* and *NbMADS4-2* genes in tobacco flowers were also identified via the VIGS (Dong et al., 2007). Furthermore, the TRV recombinant virus vector successfully induced the silencing of the *CHS* gene and *GLO1* gene in *Gerbera jamesonii* (Deng et al., 2012). In this study, we developed a VIGS system for use with perennial *Rosa* plants grown naturally in the field as experimental materials for the first time, and we used the system to study key genes of *Rosa* color and obtained results. Under conditions of the established optimal VIGS system, the petal color of both *Rosa* species was clearly lighter, which was consistent with the significantly downregulated transcript abundance of the endogenous *RrGT1* gene. The relative expression of the six key structural genes (*RrCHS*, *RrCHI*, *RrF3H*, *RrF3'H*, *RrDFR* and *RrANS*) in the upstream remained unchanged. In the biosynthetic pathway, the upstream genes are precursors for anthocyanin biosynthesis (Nakatsuka et al., 2005). Therefore, silencing of the *RrGT1* gene might lead to such a change.

The contents of eight anthocyanins, Cy3G, Cy3G5G, Pg3G, Pg3G5G, Pn3G, Pn3G5G, Dp3G and Dp3G5G, were analyzed qualitatively and quantitatively via HPLC. The results showed that the most abundant anthocyanin in the petals of *R. rugosa* 'Zizhi' was Pn3G5G, which is consistent with the results of Zhang et al. (2015). The content of Cy3G5G was the second highest, and the other anthocyanin contents were relatively low; no presence of Dp3G or Dp3G5G was detected.

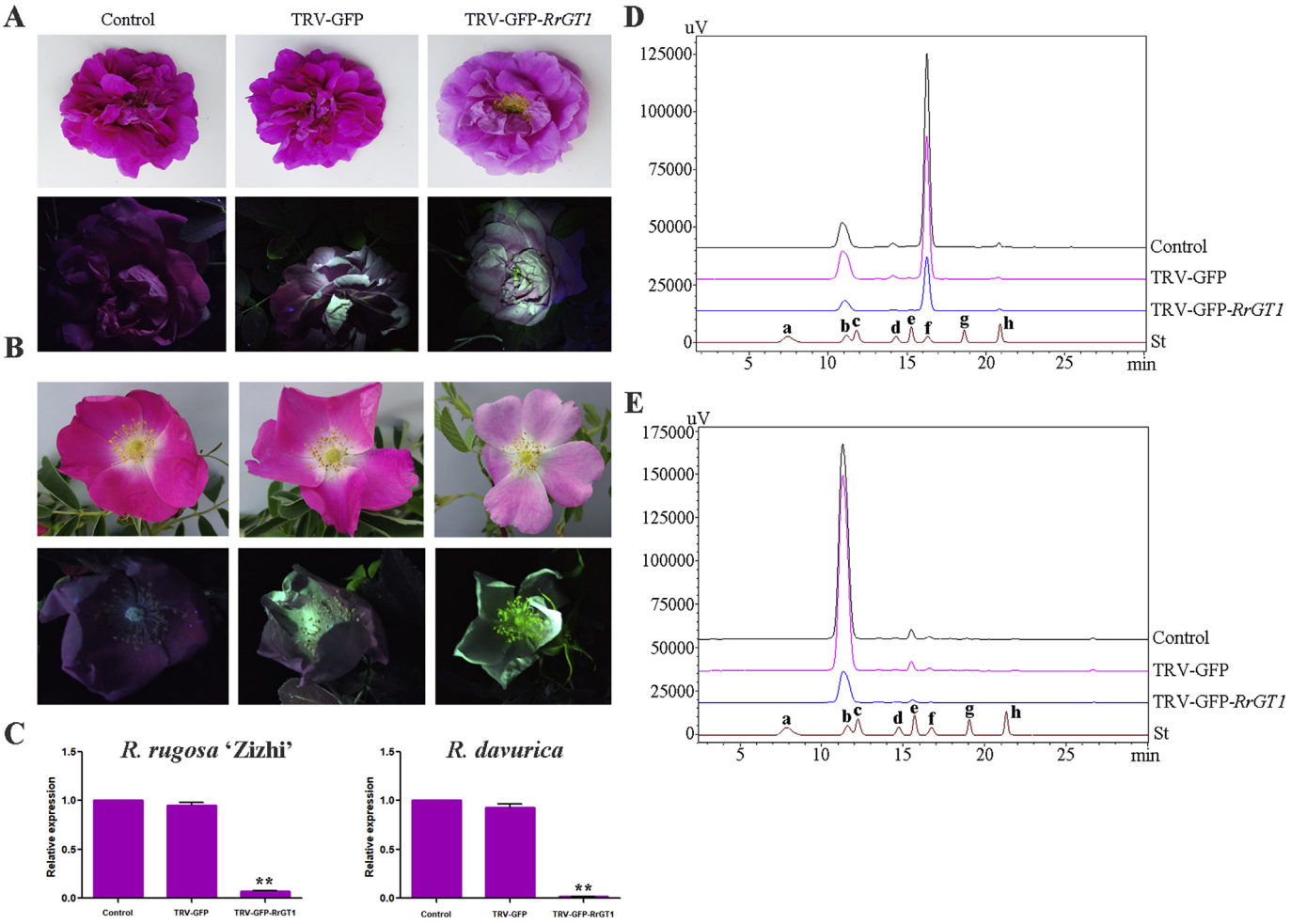

Fig. 5. Validation of VIGS in flowers. Contrast between control flowers and VIGS-treated flowers (TRV-GFP and TRV-GFP-*RrGT1*) of *R. rugosa* 'Zizhi' **(A)** and *R. davurica* **(B)**. The plants were imaged under ultraviolet illumination and normal light. **(C)** Results of the qRT-PCR detection. The error bars represent the SDs of triplicate reactions. The experiment was repeated three times, and each yielded similar results. ** indicate a significant difference from that of Control at $p < 0.01$, by Student's *t*-test. HPLC chromatograms in *R. rugosa* 'Zizhi' **(D)** and *R. davurica* **(E)**. Eight kinds of anthocyanin standards (St) were used for detection: (a) Dp3G5G; (b) Cy3G5G; (c) Dp3G; (d) Pg3G5G; (e) Cy3G; (f) Pn3G5G; (g) Pg3G; and (h) Pn3G.

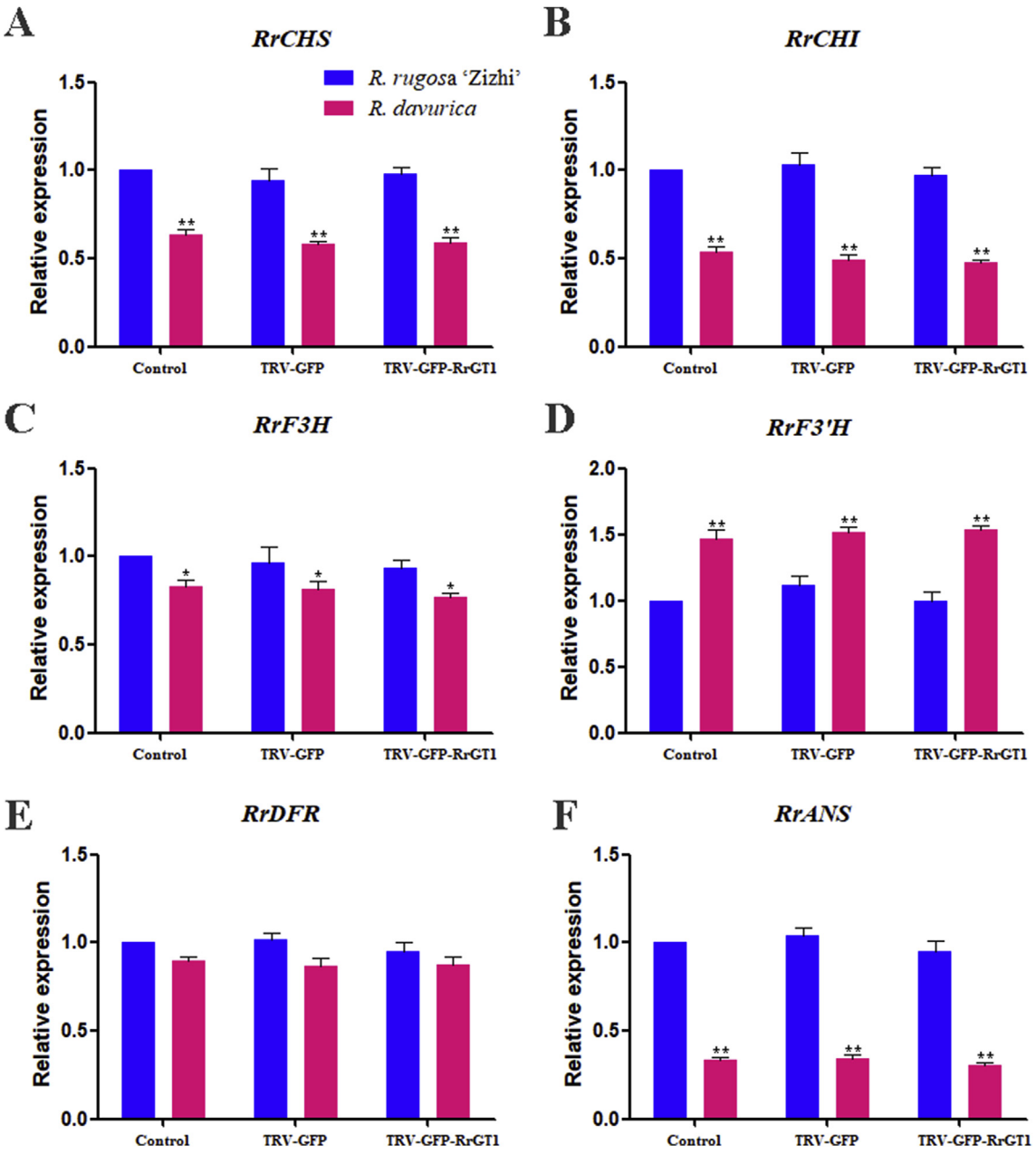

Fig. 6. The relative expression levels of the six key structural genes (*RrCHS*, *RrCHI*, *RrF3H*, *RrF3'H*, *RrDFR* and *RrANS)* in the upstream of the *RrGT1* gene in the anthocyanin pathway of *R. rugosa* 'Zizhi' and *R. davurica* at full opening stage. *RrGAPDH* was used as the internal control. The error bars represent the SDs of triplicate reactions. The experiment was repeated three times, and each yielded similar results. * and ** indicate a significant difference from that of *R. rugosa* 'Zizhi' at $P < 0.05$ and < 0.01, respectively, by Student' s *t*-test.

Table 1
Contents of anthocyanins in the flowers of *R. rugosa* 'Zizhi' and *R. davurica* subjected to different VIGS treatments (μg·g^{-1} FW).

Name	treatments	Cy3G	Cy3G5G	Pn3G	Pn3G5G	Pg3G	Pg3G5G	Dp3G	Dp3G5G
R. rugosa 'Zizhi'	Control	13.05 ± 0.04A	298.38 ± 3.85A	17.63 ± 0.12A	1773.93 ± 4.31A	5.04 ± 0.09A	52.88 ± 0.45A	–	–
	TRV-GFP	11.86 ± 0.70A	301.14 ± 1.57A	17.33 ± 0.07A	1660.26 ± 13.07B	4.82 ± 0.13A	45.32 ± 1.23B	–	–
	TRV-GFP-*RrGT1*	3.22 ± 0.12B	96.17 ± 2.22B	5.16 ± 0.06B	472.31 ± 1.28C	–	10.84 ± 0.39C	–	–
R. davurica	Control	56.72 ± 0.20A	2590.18 ± 2.45A	2.55 ± 0.03A	40.28 ± 0.09A	7.20 ± 0.01A	25.7 ± 0.36B	–	–
	TRV-GFP	55.59 ± 0.26B	2565.85 ± 3.26B	2.50 ± 0.01A	40.36 ± 0.11A	7.19 ± 0.01A	28.13 ± 0.27A	–	–
	TRV-GFP-*RrGT1*	15.33 ± 0.17C	443.17 ± 4.04C	–	1.95 ± 0.02B	0.74 ± 0.03B	6.99 ± 0.06C	–	–

* Data are the mean values ± SE of three independent replicates.Different upper case letters represent significant difference which is calculated using LSD analysis at the level of $P < 0.01$. '-' means that no corresponding anthocyanin was detected.

With respect to *R. davurica*, this is the first time different kinds and contents of anthocyanins were detected in the petals. The Cy3G5G content was dominant, that is, the coloration of *R. davurica* petals is affected mainly by Cy3G5G, while the other anthocyanins contribute little to flower color. After performing the VIGS treatment, we again carried out an HPLC analysis of both *Rosa* species. The results showed that the contents of all the different kinds of anthocyanins decreased to some extent and that the decrease in the contents of several major anthocyanins was clear in both *Rosa* species. These results are in agreement with the lighter flower color phenotypes and the relatively downregulated expression level of the endogenous *RrGT1* gene in response to VIGS treatment.

Most of the receptor substrates and donor substrates in GTs catalytic reactions are diverse. Some studies have shown that *PtUGT78L1* of poplar could catalyze the glycosylation of two or more receptors *in vitro* (Veljanovski and Constabel, 2013). Some GTs could even catalyze the glycosylation of different sites of different receptors (or the same receptor). For example, *UGT78G1* of *Medicago truncatula* could catalyze the glycosylation of 9 (iso) flavonoids compounds at different sites (Modolo et al., 2007). Combined with the current results of HPLC and previous analysis of the PSPG conserved domain of *RrGT1*, we speculated that the *RrGT1* gene was specific to the type of glycosides in the function of glycosylation. However, the selection of anthocyanins was not highly specific.

In this study, we verified and elucidated the biological functions of the *RrGT1* gene in anthocyanin metabolism in both the positive (overexpression) and negative (VIGS) directions. In conclusion, it can be inferred that *RrGT1* is a key structural gene that directly affects the formation of anthocyanins.

Author contributions

Lanyong Zhao and Zongda Xu conceived of the idea and supervised the project. Zongda Xu and Xiaoming Sui participated in designing the study, interpreting the data, and preparing the manuscript. Xiaoming Sui performed the experiments and the data analysis and drafted the manuscript. Mingyuan Zhao and Xu Han assisted in the experiments and participated in the data analysis. All authors have carefully read and approved the final version of the manuscript.

Conflicts of interest

The authors declare that they have no conflicts of interest.

Acknowledgments

This project was supported by the Agricultural Seed Project of Shandong Province ([2014] No. 96) and National Science Foundation of China (31700622).

Appendix A. Supplementary data

Supplementary data to this article can be found online at https://doi.org/10.1016/j.plaphy.2018.11.022.

References

Afifi, M., El-Kereamy, A., Legrand, V., Chervin, C., Monje, M.C., Nepveu, F., Roustan, J.P., 2003. Control of anthocyanin biosynthesis pathway gene expression by eutypine,atoxin from Eutypa lata in grape cell tiussue cultures. J. J Plant Physiol. 160, 971–975.

Bachan, S., Dinesh-Kumar, S.P., 2012. Tobacco rattle virus (TRV) based virus-induced gene silencing. Methods Mol. Biol. 894, 83–92.

Boss, P.K., Davies, C., Robinson, S.P., 1996. Anthocyanin composition and anthocyanin pathway gene expression in grapewine sports differing in berry skin colour. Aust. J. Grape Wine Res. 2, 163–170.

Broothaerts, W., Mitchell, H.J., Weir, B., Kaines, S., Smith, L.M., Yang, W., Mayer, J.E., Roa-Rodriguez, C., Jefferson, R.A., 2005. Genetransfer to plants by diverse species of bacteria. J. Nature. 433, 629–633.

Brugliera, F., Holton, T.A., Stevenson, T.W., Farcy, E., Lu, C., Cornish, E.C., 1994. Isolation and characterization of a cDNA clone corresponding to the Rt locus of Petunia hybrida. Plant J. 5, 81–92.

Burch-Smith, T.M., Schiff, M., Liu, Y., Dinesh-Kumar, S.P., 2006. Efficient virus-induced gene silencing in Arabidopsis. Plant Physiol. 142, 21–27.

Chen, J.C., Jiang, C.Z., Gookin, T.E., Hunter, D.A., Clark, D.G., Reid, M.S., 2004. Chalcone synthase as a reporter in virus-induced gene silencing studies of flower senescence. Plant Mol. Biol. 55, 521–530.

Chen, S.M., Zhu, X.R., Chen, F.D., Luo, H.L., Lv, G.S., Fang, W.M., Zhang, Z., 2010. Expression characteristics of anthocyanin structural genes in different flower color chrysanthemum cultivars. J. J. Northwest plants 3, 453–458.

Cheng, J., Wei, G., Zhou, H., Gu, C., Vimolmangkang, S., Liao, L., Han, Y., 2014. Unraveling the mechanism underlying the glycosylation and methylation of anthocyanins in peach. Plant Physiol. 166 (2), 1044.

Deng, X.B., Elomaa, P., Nguyen, C.X., Hyto"nen, T., Valkonen, J.P.T., Teeri, T.H., 2012. Virus-induced gene silencing for *Asteraceae*-a reverse genetics approach for functional genomics in *Gerbera hybrida*. Plant Biotechnology J. 10, 970–978.

Dong, Y.Y., Burch-Smith, T.M., Liu, Y.L., Mamillapalli, P., Dinesh-Kumar, S.P., 2007. A Ligation-independent cloning Tobacco rattle virus vector for high-throughput virus-induced gene silencing identifies roles for NbMADS4-1 and -2 in floral development. Plant Physiol. 145, 1161–1170.

Feng, L.G., Shao, D.W., Sheng, L.X., Zhao, L.Y., Yu, X.Y., 2009. Study on investigation and morphological variation of wild Rosa rugosa in China. J. Shandong Agric. Univ. (Nat. Sci. Ed.) 40 (4), 484–488.

Ge, C.L., Huang, C.H., Xu, X.B., 2012. Research on anthocyanins biosynthesis in fruit. Acta Hortic. Sin. 39 (9), 1655–1664.

Han, L.L., Li, J.J., Ma, Y., Guo, J., Guo, X.F., 2017. Cloning of paeonia PlGA20ox gene and expression analysis in the process of dormancy in bud. Plant Physiol. Commun. 53 (4), 677–686.

Herrera-Estrella, L., Simpson, J., 2005. Martinez-Trujillo M: Trans-genic plants: an historical perspective. J. Methods Mol Biol. 286, 3–32.

Holton, T.A., Cornish, E.C., 1995. Genetics and biochemistry of anthocyanin biosynthesis. Plant Cell 7, 1071.

Jiang, C.Z., Chen, J.C., Reid, M., 2011. Virus-induced gene silencing in ornamental plants. Methods Mol. Biol. 744, 81–96.

Ju, Z.G., 1995. Activities of chalcone and UDP Gal: flavonoid-3-O-glycosyhransferase in relation to anthocyanin synthesis in apple. J. Sci Horticulturae. 63, 175–185.

Kim, S.H., Lee, J.R., Hong, S.T., Yoo, Y.K., An, G., Kim, S.R., 2003. Molecular cloning and analysis of anthocyanin biosynthesis genes preferentially expressed in apple skin. Plant Sci. 165, 403–413.

Kobayashi, S., Ishimaru, M., Ding, C.K., Yakushiji, H., Goto, N., 2001. Comparison of UDP-glucose:Flavonoid 3-O-glucosyltransferase (UFGT) gene sequences between white grapes (*Vitis Vinifera*) and theirsports with red skin. J. Plant Sci. 160, 543–550.

Kroon, J., Souer, E., de Graaff, A., Xue, Y., Mol, J., Koes, R., 1994. Cloning and structural analysis of the anthocyanin pigmentation locus Rt of Petunia hybrida: characterization of insertion sequences in two mutant alleles. Plant J. 5, 69–80.

Kubo, A., Arai, Y., Nagashima, S., Yoshikawa, T., 2004. Alteration of sugar donor specificities of plant glycosyltransferases by a single point mutation. J. Arch Biochem Biophys. 429 (2), 198–203.

Li, X.G., Yu, Z.Y., 2003. Research progress of anthocyanin. J. Northern horticulture. 4, 6–8.

Liu, Y., Schiff, M., Dinesh-Kumar, S.P., 2002. Virus-induced gene silencing in tomato. Plant J. 31, 777–786.

Martens, S., Preuß, A., Matern, U., 2010. Multifunctional flavonoid dioxygenases: flavonol and anthocyanin biosynthesis in Arabidopsis thaliana. L. Phytochemistry. 71, 1040–1049.

Martin, R.C., Mok, M.C., Habben, J.E., Mok, D.W.S., 2001. A maize cytokinin gene encoding an O-glucosyltransferase specific to cis-zeatin. Proc. Natl. Acad. Sci. U.S.A. 98, 5922–5926.

Martin, R.C., Mok, M.C., Mok, D.W.S., 1999. Isolation of a cytokinin gene, ZOG1, encoding zeatin O- glucosyltransferase from Phaseolus lunatus. Proc. Natl. Acad. Sci. U.S.A. 96, 284–289.

Modolo, L.V., Blount, J.W., Achnine, L., Naoumkina, M.A., Wang, X., Dixon, R.A., 2007. A functional genomics approach to (iso) flavonoid glycosylation in the model legume Medicago truncatula. J. Plant molecular biology. 64 (5), 499–518.

Modolo, L.V., Li, L.N., Pan, H.Y., Blount, J.W., Dixon, R.A., Wang, X.Q., 2009. Crystal structures of glycosyltransferase UGT/8G1 reveal the molecular basis for glycosylation and deglycosylation of (iso) flavonoids. J. J Mol Biol. 392 (5), 1292–1302.

Nakatsuka, T., Nishihara, M., Mishiba, K., Yamamura, S., 2005. Two different mutations are involved in the formation of white-flowered gentian plants. J. Plant Sci. 169, 949–958.

Qi, Y., 2016. Cloning and Expression Analysis of Anthocyanin Biosynthesis Related Gene in *Rosa rugosa*. Shandong agricultural university.

Quadrana, L., Rodriguez, M.C., López, M., Bermúdez, L., Nunes-Nesi, A., Fernie, A.R., Descalzo, A., Asis, R., Rossi, M., Asurmendi, S., Carrari, F., 2011. Coupling virus-induced gene silencing to exogenous green fluorescence protein expression provides a highly efficient system for functional genomics in Arabidopsis and across all stages of tomato fruit development. Plant Physiol. 156 (3), 1278–1291.

Schmittgen, T.D., Livak, K.J., 2008. Analyzing real-time PCR data by the comparative C(T) method. Nat. Protoc. 3 (6), 1101.

Spitzer, B., Zvi, M.M.B., Ovadis, M., Marhevka, E., Barkai, O., Edelbaum, O., Marton, I., Masci, T., Alon, M., Morin, S., Rogachev, I., Aharoni, S., Vainstein, A., 2007. Reverse Genetics of floral scent: application of Tobacco rattle virus-based gene silencing in Petunia. Plant Physiol. 145, 1241–1250.

Sun, D., Nandety, R.S., Zhang, Y., Reid, M.S., Niu, L., Jiang, C.Z., 2016. A petunia

ethylene-responsive element binding factor, PhERF2, plays an important role in antiviral RNA silencing. J. Exp. Bot. 67, 3353–3365.
Szerszen, J.B., Szczyglowski, K., Bandurski iaglu, R.S., 1994. A gene from Zea mays involved in conjugation of growth hormone indole-3-acetic acid. Science 265, 1699–1700.
Veljanovski, V., Constabel, C.P., 2013. Molecular cloning and biochemical characterization of two UDP-glycosyltransferases from poplar. J. Phytochemistry. 91, 148–157.
Vogt, T., Jones, P., 2000. Glycosyltransferases in plant natural product synthesis: characterization of a supergene family. Trends Plant Sci. 5, 380–386.
Wang, C.X., Yang, M.Z., Pan, N.S., Chen, Z.L., 1993. Resistance to potato virus X infection in transgenic tobacco plants with coat protein gene of virus. J. Journal of Integrative Plant Biology. 35 (11), 819–824.
Wang, X.Q., 2009. Structure, mechanism and engineering of plant natural product glycosyltransferases. J. FEBS Lett. 583 (20), 3303–3309.
Yang, Q., Yuan, T., Sun, X.B., 2015. Preliminary studies on the changes of flower color during the flowering period in two tree peony cultivars. Acta Hortic. Sin. 42 (5), 930–938.
Yonekura-Sakakibara, K., Hanada, K., 2011. An evolutionary view of functional diversity in family 1 glycosyltransferases. J. Plant J. 66 (1), 182–193.
Zhang, L., Xu, Z.D., Tang, T.F., Zhang, H., Zhao, L.Y., 2015. Analysis of anthocyanin related compounds and metabolic pathways in the flowering process of Rosa rugosa 'Zizhi'. China agricultural science 48 (13), 235–236.
Zhang, X.Y., Xue, Q.Z., 2001. Introduction of soybean glycinin gene into rice (Oryza sativa L.) with Agrobacterium-mediated transformation. J. Journal of Zhejiang Agricultural University(Agric.& Life Sci.). 27 (5), 495–499.